2011-01-01

Application of Niobium Enriched Ormosils as Thermally Stable Coatings for Aerospace Aluminium Coatings

P.C. Rajath Varma
Technological University Dublin, rajath.varma@tudublin.ie

Mohamed Oubaha
Dublin City University

Pradeepan Periyat
University of Limerick, ppnambiar@gmail.com

Colette McDonagh
Dublin City University

Brendan Duffy
Technological University Dublin, brendan.duffy@tudublin.ie

Recommended Citation

Varma, R. et al. (2011) Application of Niobium Enriched Ormosils as Thermally Stable Coatings for Aerospace Aluminium Coatings. *Surface and Coatings Technology,* Volume 205, Issue 16, 15 May 2011, pp. 3992-3998. doi:10.1016/j.surfcoat.2011.02.023

Application of niobium enriched ormosils as thermally stable coatings for aerospace aluminium alloys.

P.C. Rajath Varma[a], Pradeepan Periyat[b], Mohamed Oubaha[c], Colette McDonagh[c], Brendan Duffy[a]*

[a] Centre for Research on Engineering Surface Technology (CREST), FOCAS Institute, Dublin Institute of Technology, 13 Camden Row, Dublin 8, Ireland

[b] Materials and Surface Science Institute (MSSI), University of Limerick, Limerick Co. Ireland.

[c] National Centre for Sensor Research (NCSR), Dublin City University, Dublin 9, Ireland

Abstract

The aim of this experimental research is to study the ability of niobium rich sol-gel coatings to withstand thermal stress, while remaining impermeable to corrosive agents for the protection of aerospace alloys. The coating material is developed via polymeric sol-gel synthesis employing 3-(trimethoxysilyl)propylmethacrylate (MAPTMS) and niobium ethoxide precursors as a source of silicon and niobium, respectively. The beneficial effect of niobium inclusion within coating was characterised spectroscopically, calorimetrically and electrochemically. The thermal cycling effects of the coating were studied using microscopic and accelerated test methods. Electrochemical tests showed that corrosion current of the material was 2 orders lower in magnitude than MAPTMS coating. The neutral salt spray test results of thermal stressed samples prove that inclusion of niobium nanoparticles within the silane matrix considerably improves the corrosion resistance performances in salt spray test resulting in better ability to resist thermal shock failure when compared to the MAPTMS coating alone.

Keywords: Sol-Gel; Thermal cycling; Aluminium Alloy; Corrosion.

---

*Corresponding author. Tel.: +353 1 402 7964; fax: +353 1 402 7941.
E-mail address: bduffy@dit.ie (Brendan Duffy).

1 Introduction

Niobium precursors have emerged as another range of useful sol-gel materials for engineering applications. Niobium has attracted attention due to the corrosion resistance properties and thermodynamic stability of niobium oxide, particularly as a coating material for biomedical applications [1]. Excellent corrosion resistant properties have led Marchus et al. to patent a chemical conversion coating developed using niobium compounds for the protection of magnesium alloys [2]. Niobium-silicon mixed-oxide composites synthesized by the sol-gel method have also attracted great interest for their potential applications such as heterogeneous catalysts [3, 4], supports for bio-molecule immobilization [3, 5] and energetic materials [6].

The sol-gel process is an interesting route to obtain composite coatings taking into account its relative simplicity and low cost. There are excellent literature manuscripts [7-12] and books [13] available which describe the chemistry of the sol-gel process involved in the development of a wide range of materials. The applications and opportunities for sol-gel in engineering purpose have relied on the ability to synergistically combine various chemistries. Organic-inorganic materials synthesised at room temperature via a sol-gel route are particularly attractive for anti-corrosion protection applications as they combine the advantages of organic polymers (ease of processing, mechanical properties, new functionality by incorporation of organic or inorganic moieties) with the characteristics of inorganic oxides (hardness, thermal and chemical stability, transparency). The most common sol-gels used for coatings are organically modified silicates (Ormosils) which are formed by the hydrolysis and condensation of organically modified silanes with alkoxide precursors [14, 15]. Alkoxysilanes, such as tetraethoxysilane (TEOS) and alkoxides of zirconium [9], titanium [16] and aluminium are commonly used in the sol-gel route to prepare corrosion protective coatings and other engineering purposes [9]. The sol composition and the heat treatment used controls respectively the

relative composition of the deposited components (dopant, mixed oxide) as well as their crystalline or amorphous nature of their microstructures.

When ice accretions during cold climate at critical locations (trailing edges of wings, tails, rotors, inlets, etc.) of an aircraft can affect aerodynamic properties, reducing engine performance and stability. Current de-icing processes involve the use high-velocity water, steam, or de-icing fluid for removing large masses of ice from the aircraft components [17]. This may cause the aircraft coatings to experience a thermal shock, or stress, which may lead to crack formation in coating and thereby decreasing its barrier properties.

This work is aimed to develop a coating for aerospace alloy AA 2024-T3 which will show excellent barrier properties after undergoing a thermal stress process. The coatings were synthesized using niobium ethoxide (NbOEt), and 3-(trimethoxysilyl) propylmethacrylate (MAPTMS). Methacrylic acid is used as chelating agent in order to prevent rapid hydrolysis of Nb^{+5} ions and thus the formation of hydrated niobium pentoxide precipitate. The sol-gel was then deposited on AA 2024-T3 substrate by spin coating. The physical properties of the sol-gel material were studied using differential scanning calorimetry (DSC) and dynamic light scattering (DLS). X-ray photoelectron spectroscopy (XPS) was used to study the chemical compositions of the sol-gel coating, while scanning electron microscope (SEM) and atomic force microscopy (AFM) were used to study the surface morphology. The electrochemical behaviour of the coatings was studied using potentiodynamic scanning (PDS). Neutral salt spray test of the thermal cycled samples was used to study the coating performance in accelerated corrosion atmosphere. The properties of hybrid coating were then compared to MAPTMS coating alone. The results proves that the inclusion of niobium in the silane coatings improves the coating performance, especially in harsh environments where aluminium alloys are dependant on protective coatings for long term usage.

2 Experimental

2.1 Synthesis of sol-gel

The sols were prepared according to the experimental schematic in Fig. 1. The silane precursor, 3-(trimethoxysilyl)propylmethacrylate (MAPTMS) (Sigma Aldrich, Irl, Assay ~99%) was pre-hydrolysed using 0.01 N HNO_3 for 45 min (A). Simultaneously, niobium ethoxide (NbOEt) (Sigma Aldrich, Irl) was chelated using methacrylic acid (Sigma Alrich, Irl), at a 1:1 molar ratio for 45 minutes (B). All the chemicals were used without further modification. Solution A was slowly added to solution B over ten minutes. The mixture of A with B is characterized by an exothermic reaction indicating a chemical reaction, rather than a physical dispersion was occurring. Following another 45 min, water (pH 7) was added to this mixture to give a final molar ratio of 2.5:1:1:5 (MAPTMS: Ligand: NbOEt: H_2O), as used previously [18].

Fig.1

For comparative purposes a MAPTMS sol-gel was prepared by combining the silane precursor MAPTMS precursor, dilute HNO_3 (aq) as catalyst, ethanol as solvent and water for hydrolysis with a molar ratio of 1:0.001:2.5:5 (MAPTMS: HNO_3: ETOH: H_2O). All the reaction mixtures were stirred overnight to complete the reaction. All chemicals were used as received.

For description purposes the final sol-gel coating materials will be referred in shorthand notation as MAPTMS and for niobium containing coatings; MAPTMS/Nb.

2.2 Preparation of sol-gel coating

AA2024-T3 aluminium panels (150 mm x 100 mm) were sourced from Amari Irl, Clondalkin. The panels were degreased with isopropanol, alkaline cleaned using Oakite 61 B® (Chemetall, UK) by immersion at 60ºC for 1 minute and washed in warm deionised water. The sol-gel solutions were filtered using a 0.45 μm syringe filter and applied by spin coating on AA 2024-T3 alloy at up to 1000 rpm and cured for 12 hr at 100°C to obtain a touch dry finish. The final thickness of MAPTMS and MAPTMS/Nb coating was 2 ± 0.7 μm and 4 ± 0.5 μm respectively, as measured using an Elcometer® non destructive coating thickness gauge.

2.3 Differential scanning calorimetry

DSC measurements were carried out using a Shimadzu DSC QC instrument under an air atmosphere at a heating rate of 10°C/min between 50 and 350°C, although the working temperature for a typical hybrid sol-gel coating would be likely below 250ºC [16]. Samples were prepared by dropping 10 μl of the prepared solution into aluminium sample pans and curing at 100° C for 1 hr in an oven.

2.4 Particle size analysis

Sol-gel particle sizes were determined using a Malvern Nano-ZS instrument, using the Dynamic light scattering (DLS) technique. The technique is a well-established optical method used to study dynamic processes of liquids and solids. The experiment was conducted at an ambient temperature.

2.5 XPS studies

X-ray Photoelectron Spectroscopy (XPS) analyses were performed to study the chemical state of niobium in the coating using a Krats AXIS 165 spectrometer. The instrument employs a monochromated Al Kα X-ray source ($h\nu$ = 1486.58 eV) which was used at 150 W (10 mA, 15kV).

For survey spectra, pass energy of 160 eV was used. For high resolution spectra of C1s, O1s, Si2p and Nb3d, pass energy of 20 eV was used.

2.6 AFM studies

The morphology of the sol-gel films was assessed by AFM using an Asylum MFP-3D AC microscope, fitted with an aluminium coated silicon tip at a scan rate of 0.7 Hz. Damage to the tip and sample surface was minimised by running the experiment in tapping mode. The surface roughness values (R_a) are calculated with inbuilt AFM software using root mean square values of surface height measurements over an area of 25μm^2.

2.7 Electrochemical studies

The electrochemical data was obtained using a Solartron SI 1287/1255B system comprising of frequency analyser and potentiostat. Potentiodynamic scanning was performed using an electrochemical cell (PAR K0235 Flat Cell) with an exposed area of 0.78cm^2 in Harrison's solution (3.5 wt% $(NH_4)_2SO_4$ and 0.5 wt% NaCl) where the coated metal acted as a working electrode, a silver/silver chloride (Ag/AgCl) electrode was used as a reference electrode and platinum mesh as a counter electrode. All scans were acquired in the region from -0.8 V to + 0.8 V vs. open circuit potential (E_{oc}), with a scan rate 1 mV/sec at room temperatures (20 °C ± 2 °C).

2.8 Thermal stress testing

Thermal stressing consisted of cycling a sample between two extreme temperatures which are held for a fixed amount of time for a specified number of cycles. As samples heat up and cool down they expand and contract, potentially causing stress or adhesion failure of the coating over time. The sol-gel coated samples were thermally cycled between a -45 (± 5) °C and 245 (± 5) °C for dwell time of 30 mins with 10 cycles as recommended by an aerospace manufacturer (BS EN 4170:2007). The thermal stability of the coatings were examined using a modified version of the aerospace standard for paints and varnishes.

2.9 Neutral salt spray (NSS) exposure

The samples were exposed to salt fog atmosphere generated from 5 wt% aqueous NaCl solution at 35 (± 1) °C for 168 hours according to ASTM B117 specifications [19]. The non coated side and edges of the panels were protected using water a based polyurethane coating (Alberdink®). The edges were further protected with 3 M insulation tapes.

3 Result and Discussion

3.1 Particle size analysis using DLS and FE-SEM

Particle size measurements of both sol-gel materials using DLS technique (Fig. 2) indicate the formation of two different particles in MAPTMS/Nb (0.8 and 3.5 nm), when compared to one peak in MAPTMS sol-gel located at ~3nm.

These results indicate that the MAPTMS/Nb material is not composed of a homogenous molecular or oligomeric system, but clearly reveals the presence of two very distinct systems. As the peak located at ~3.5nm is located in a size region close to the one observed for the MAPTMS material, one can suspect that it is related to the organosilane species and conclude the one observed at 0.8nm related to the niobium particles, which can be attributed to Nb_2O_5 like nanoparticles. The difference in size nanoparticles between MAPTMS/Nb and MAPTMS can be explained by the catalysis of the condensation of the silanol groups into siloxanes groups in presence of strong nucleophilic groups such as metal transition complexes, as previously demonstrated in similar molecular systems [18].

Fig. 2

SEM was used in order to analyse the coatings and to confirm the presence of artifacts/defects such as nanoparticles/ cracks. SEM observations (Fig. 3) confirm the presence of uniformly distributed nanoparticles of sizes between 100 and 200 nm in both sol-gel coatings on AA 2024-T3 substrate

resulting from particle growth during the curing process. The increased presence of the particles in MAPTMS/Nb can be attributed to the formation and growth of silicon-niobate microstructures.

Fig. 3

3.2 Thermal stability

Fig. 4 shows both the DSC curves of MAPTMS and MAPTMS/Nb materials. First, it can be observed that the inclusion of the niobium complex within the organosilane matrix increases the glass transition temperature by about 60 ºC to 220 ºC, when compared to MAPTMS (T_g =160 ºC). Second, the MAPTMS/Nb DSC curve exhibits an additional large exothermic peak at 325 ºC, whereas MAPTMS exhibits a single large peak observed at 160 ºC. The increase of the T_g can be explained by an increase of the molecular interactions with the material. From a molecular structure point of view, these differences can be primarily explained by an increase in the level of connectivity of the network between the organic and the inorganic species. Indeed, two different chemical reactions can happen both contributing to the density and the thermal stability of the global material. The niobium complex can form Nb-OH groups via hydrolysis reaction with water, which in theory can either auto condense to form an Nb_2O_5 like structure, dispersed within the organosilane matrix forming a molecular composite material, or condense with the residual silanol groups located on the MAPTMS, then forming a molecularly homogeneous material composed of Si-O-Nb covalent bonds. However, to our knowledge, no such study has highlighted either the specificity or the prevalence of any of the above mentioned reactions.

Fig. 4

3.3 XPS analysis

XPS analysis was performed aiming at identifying the chemical composition of the particles observed on the coating surface (Table 1). There was evidence in both coatings (MAPTMS and MAPTMS/Nb) of silicon, oxygen and carbon while the presence of niobium was confirmed in the MAPTMS/Nb coating. The high resolution XPS spectrum of O1s and Nb 3d were presented in Fig. 5.

The total amount of the niobium present in the sample was found to be 1.8 At%, where the 1.1 At.% contribution came from Nb $3d_{5/2}$ spin-orbit component and 0.7 At% are from second spin-orbit component Nb $3d_{3/2}$. This is represented by sharp doublet peaks at 207.7 and 210.5 eV, characteristically of Nb_2O_5 particles [20]. Table 1 show that the amount of Si, C, O and Nb presented in the MAPTMS and MAPTMS/Nb. The ratio of MAPTMS/Nb was found to be 9:2, indicating that the sol is homogenously dispersed.

Table 1

Fig. 5

3.4 AFM studies

Fig. 6 (a) & (b)

AFM was used for characterizing the surface topography of all the sol-gel coated AA-2024 T3 substrates before and after the thermal cycling test (Fig. 6 & Fig. 7). The AFM image of the MAPTMS coating (Fig 6 (a)) detected the presence of pores widespread with an average pore size 1.10 nm (± 0.05 nm) along with few particles on the surface with a surface roughness of 0.67 nm. Nanoparticles were also detected for MAPTMS/Nb coating (**Error! Reference source not found.**

(b)) which can be attributed to Nb_2O_5 and SiO_2 particles. The surface morphology of MAPTMS/Nb also displayed higher packing levels with very few pores or if any with average pore size of ~ 0.3 nm and a surface roughness value of 0.55nm.

Fig. 7 (a) & (b)

AFM images (Fig. 7) of samples after the thermal stressing process revealed a clear difference in surface pattern of the sol gel coated samples. Exposure to higher temperature of sol-gel coating has resulted in particle growth which is clearly seen in both coatings. Another effect of the thermal stressing process is also seen as surface roughness values increased for both coatings. It is interesting to note that the surface roughness of MAPTMS (R_a=1.53 nm, Fig. 7(a)) is nearly twice when compared to MAPTMS/Nb coating (R_a= 0.75 nm, Fig. 7(b)) coating after thermal cycling. This shows that the presence of niobium nano particle may have a mutual effect on the particle growth of SiO_2 and Nb_2O_5 nanoparticles.

3.5 Potentiodynamic scan studies

Polarisation methods, such as potentiodynamic scanning are often used for laboratory based corrosion testing as they provide useful information on the corrosion mechanisms, corrosion rate and susceptibility of specific materials to corrosion in designated environments [21, 22].

Using Harrison's solution, potentiodynamic evaluation involved applying a voltage from 0.8 V below the open circuit potential (cathodic region) to 0.8 V above it (anodic region). Therefore the degree of change in the current density (electron exchange occurring at the electrodes) is a function of the potential applied. If a high enough potential (overpotential) is applied then corrosion is forced, so a coating that maintains a low current density at high overpotential is desirable. The Corrosion protection properties such as corrosion current densities (I_{corr}) and potential (E_{corr}) were estimated by

the Tafel method [23], while the polarisation resistance (R_{pol}) was calculated using Stern-Geary equation [24] (Eqn 1)

$$I_{corr} = B / R_{pol} \qquad \text{(Eqn 1)}$$

Where R_{pol} is the polarisation resistance and B is proportionality constant for the particular system which is calculated from and the slopes of the anodic (β_a) and cathodic (β_c) Tafel regions as shown by Eqn. 2.

$$B = \frac{\beta_a . \beta_c}{2.303(\beta_a + \beta_c)} \qquad \text{(Eqn 2)}$$

Potentiodynamic scans for bare and sol-gel coated AA 2024-T3 are shown in Fig. 8. It should be noted that as the solution was agitated by aeration and not stirring. As the metallic surface is covered by a coating, the rate determining step of the electrode process is probably not the activation of that charge transfer and thus, the physical values in Table 2 can only be used to differentiate the samples qualitatively, but not quantitatively.

The potentiodynamic polarization of the bare aluminium alloy exhibits no obvious passivation region and the current density initially increases rapidly above its open circuit potential because an active electrochemical reaction has occurred on the surface. A similar type of behaviour is seen for MAPTMS coating, with a higher corrosion potential (E_{corr}= 0.450 V) when compared to bare substrate (E_{corr}= 0.580 V).

MAPTMS/Nb displays a lower current densities in both the anodic and cathodic branches of the polarization curves, indicating that the anodic ($Al \rightarrow Al^{3+} + 3e^-$) and cathodic ($O_2 + 2H_2O + 4e^- \rightarrow 4OH$) processes are inhibited simultaneously. The polarisation resistance was also found to be higher for

MAPTMS/Nb coating by 3 orders in magnitude (R_{pol} = 2.83 x 10^6 Ω. cm^2) when compared to MAPTMS coating (R_{pol} = 8.20 x 10^3 Ω. cm^2). Therefore it is proposed that the presence of Nb_2O_5 nanoparticles increased the network condensation, improving cross-linking and thus forming a denser film than the MAPTMS coating.

Fig. 8

Table 2

3.6 Neutrals salts spray test results of thermal stressed panels

The thermal stresses induced are similar to those experienced by aerodynamical surfaces where hot deicing fluids are used to remove ice accretion on wing sections. The panels were tested for barrier properties after thermal cycling, where it was found that all coatings remained intact. The results from neutral salt spray exposure for the thermally stressed sol-gels coated AA 2024-T3 panels are shown in Fig 9. Failure of a coating was defined as being three or more pits per panel (adapted from the BS EN ISO-10289 standard) or coating delamination. Panels were inspected at 24 hr intervals. The pit formation on MAPTMS coating started between 24 to 48 hr of exposure and with extensive corrosion product formation (Fig. 9(A)) after 168 hr. For MAPTMS/Nb coated samples first sight of pit formation at two different areas (marked in red in Fig 9 (B)) was started to appear after 72 hr with no further damage up to 168 hr. Some pinholes (<10) were also seen for MAPTMS/Nb coating. The result revealed that niobium inclusion into the silane matrix shows better barrier properties when compared to MAPTMS coating on AA 2024-T3. The improved performance of MAPTMS/Nb coating may be due to its resistance to thermal shock. Thermal shock failure may occur due to single or rapid temperature changes or as are result of cyclic temperature changes which introduce enough stresses to cause a failure such as cracking or coating delamination. Literature studies confirm an increase in coefficient of thermal expansion (CTE) and decrease in thermal conductivity can reduce a materials resistance to thermal shock [25]. The presence SiO_2 and Nb_2O_5 content will effectively

decrease CTE of composite films or metal surfaces during either oxidation or thermal cycling [26, 27]. Therefore an improved barrier property after salt spray test would be expected for MAPTMS/Nb coating when compared to MAPTMS due to the presence of both SiO_2 and Nb_2O_5 nanoparticles.

Fig. 9

4 Conclusion

Organosilane based materials were synthesized using the sol-gel routes and applied on aerospace alloy AA 2024-T3 panels. The particle size study using DLS study and SEM images shows that particles were present in both coatings. DSC study confirmed higher thermal stability for MAPTMS/Nb when compared to MAPTMS. AFM studies of the sol-gel coatings displayed a clear difference in surface topography of the sol-gel coating before and after thermal stressing. The presence of niobium in the silane coating seems to have an effect on the particle growth during the thermal cycling process. The electrochemical studies prove that the inclusion of nobium into the silane matrix significantly improved the corrosion protection properties of the ormosil coating. The improved performance of the niobium inclusion can be attributed to the formation of denser polymer during the hydrolysis and condensation process thus providing a strong and robust polymer network when applied as coating. The neutral salt spray result revealed that the niobium inclusion has improved the corrosion protection of thermal stressed MAPTMS/Nb coating over MAPTMS by improving its thermal shock properties. The thermal shock resistant property exhibited by niobium rich silane makes it an ideal candidate for aerospace trailing edge coatings where hot fluid treatment is used to remove ice accretions.

Acknowledgement

The authors would like to thank Enterprise Ireland for financial support through the Dualion project (CFTD/05/306). The authors are indebted to Anne Shanahan and Dr. Luke O'Neil for their excellent SEM and AFM assistance.

5 Reference

[1] D. Velten, E. Eisenbarth, N. Schanne, J. Breme, J. Mater. Sci. Mater. Med. 15 (2004) 457.

[2] P. Marcus, H. Ardelean, Patent PCT/FR 02/01843, WO 02/097164 A2, 2002, US Patent 7 156 905, 2007.

[3] A. Aronne, E. Marenna, V. Califano, E. Fanelli, P. Pernice, M. Trifuoggi, A. Vergara, J. Sol-Gel Sci. Technol. 43 (2007) 193.

[4] M.S.P Francisco, R. Landers, Y. Gushikem, J. Solid State Chem. 177 (2004) 2432.

[5] S.S. Rosatto, P. T. Sotomayor, L. T. Kubota, Y. Gushikem, Electrochim. Acta 47(2002) 4451.

[6] B. J Clapsaddle, D.W Sprehn, A.E Gash, J.H Satcher Jr, R.L Simpson J Non-Cryst Solids 350 (2004)173.

[7] J. Livage, M. Henry and C. Sanchez, Prog. Solid State Chem. 288 (1988) 259.

[8] C. J. Brinker and G. Scherrer, Sol-Gel Science: The Physics and Chemistry of Sol-Gel Processing, Academic Press, San Diego, CA, 1990.

[9] L. L. Hench and J. K. West, Chem. Rev. 93 (1990) 33.

[10] M.L. Zheludkevich, I. Miranda Salvado, M.G.S. Ferreira, J. Mater. Chem. 15 (2005) 5099.

[11] M. Guglielmi, J. Sol-Gel Sci. Technol. 8 (1997) 443.

[12] C. Sanchez, B. Julian, P. Belleville, M. Popall, J. Mater. Chem. 15 (2005) 3559.

[13] Sanchez, Romero (Eds), Functional Hybrid Materials, Wiley-VCH, Weinheim, ISBN-13: 978-3-527-30484-4.

[14] R.L. Parkhill, E.T. Knobbe, M.S. Donley, Prog. Org. Coat. 41 (2001) 261.

[15] R. Kasemann, H. Schmidt, First European Workshop on Hybrid Organic-Inorganic Materials, Chateau de Bierville, France, 8-10 November, 1993, p. 171.

[16] S.V. Lamaka, M.L. Zheludkevich, K.A. Yasakau, R. Serra, S.K. Poznyak, M.G.S. Ferreira Prog. Org. Coat. 58 (2007) 127.

[17] C. C. Ryerson, Cold Reg. Sci. Technol. (2010), doi:10.1016/j.coldregions.2010.02.006.

[18] P.C. Rajath Varma, J. Colreavy, J. Cassidy, M. Oubaha, B. Duffy, C. McDonagh, Prog. Org. Coat. 66 (2009) 406.

[19] ASTM B117, Annual Book of ASTM Standards, Philadelphia, USA, 1997.

[20] H. Ardelean, I. Frateur, P. Marcus, Corros. Sci. 50 (2008) 1907.

[21] D.A. Jones, "Principles and Prevention of Corrosion", Prentice-Hall Inc., New Jersey, (1996).
[22] J.C. Scully, "The Fundamentals of Corrosion", 3rd edition, Pergamon Press (1990).
[23] M. Kendig, S. Jeanjaquet, R. Addison, J. Waldrop, Surf. Coat. Technol. 140 (2001) 58.
[24] V. Barranco, S. Feliu Jr, S. Feliu, Corr. Sci. 46 (2004) 2203-2220.
[25] J. R. Davis, "Heat Resistant materials", 2nEd. ASM International, OH, USA 1997 p 205
[26] Zheng-dao Wang, J. J. Lu, Y. Li, S.Y. Fu, S. Jiang, X. X Zhao, Composites: Part A 37 (2006)74.
[27] D. L. Douglass, J. Less-Common Met. 5 (1963) 151.

List of Tables

Table 1: Amount of silicon, carbon, oxygen and niobium present in the sol-gel coating (amount are in At. %).

Coating Sample	Silicon	Carbon	Oxygen	Niobium
MAPTMS	8.6	61.5	29.9	-
MAPTMS/Nb	7.8	57.8	32.7	1.8

Table 2: Corrosion parameters estimated from potentiodynamic scan for bare AA 2024-T3 and sol-gel coatings

Sol-gel coatings	I_{corr} (A/cm^2)	E_{corr} (V)	$\|\beta a\|$ (V/decade)	$\|\beta c\|$ (V/decade)	R_{pol} (Ω. cm^2)
Bare AA 2024-T3	3.91×10^{-7}	-0.580	0.037	0.086	1.33×10^{3}
MAPTMS	3.43×10^{-7}	-0.450	0.052	0.694	8.20×10^{3}
MAPTMS/Nb	1.54×10^{-9}	-0.504	0.231	0.297	2.83×10^{6}

List of Figures:

Fig. 1

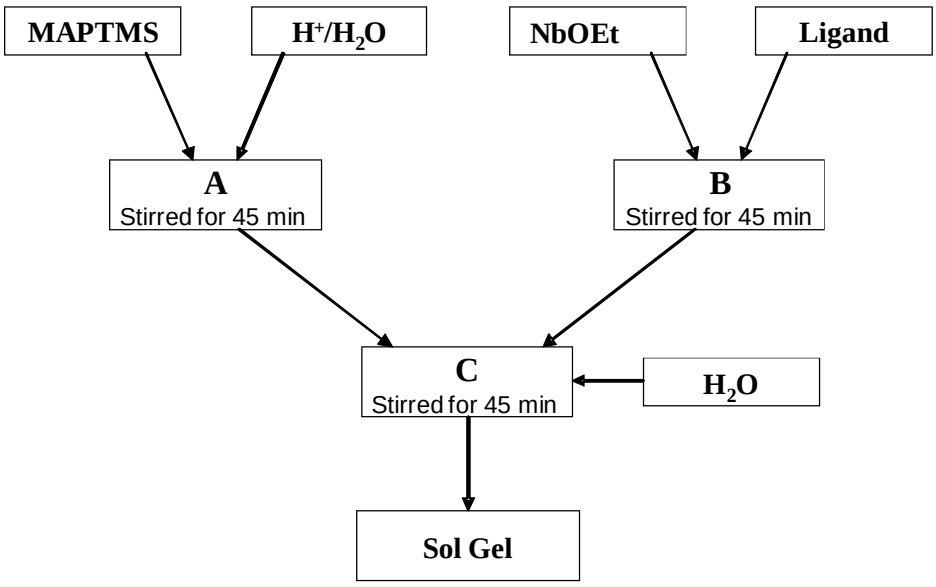
MAPTMS
H+/H2O
NbOEt
Ligand
A
Stirred for 45 min
B
Stirred for 45 min
C
Stirred for 45 min
H2O
Sol Gel

Fig. 2

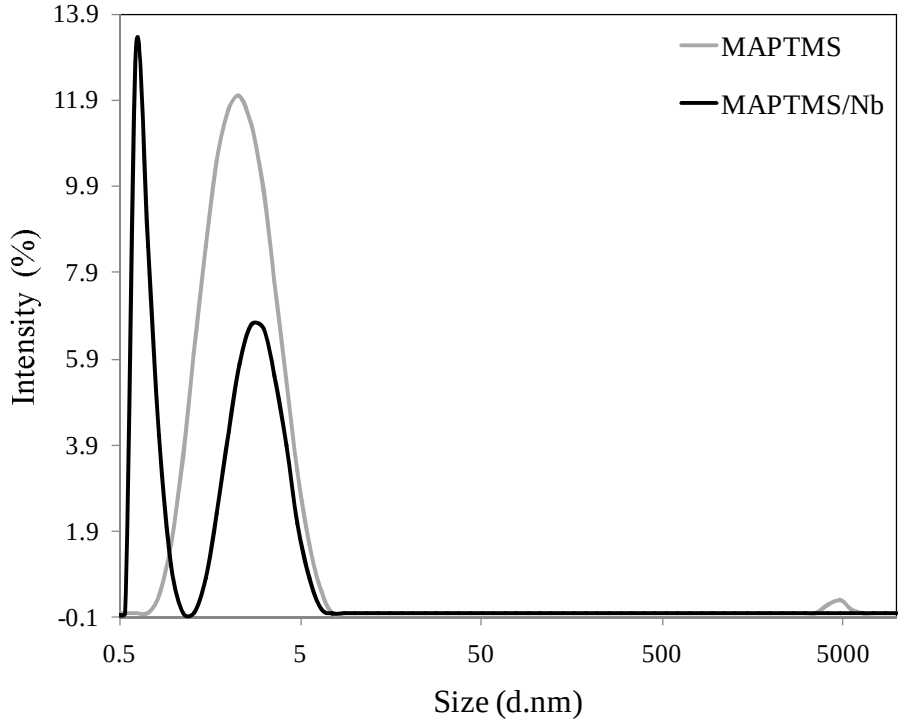
13.9
11.9
9.9
7.9
5.9
3.9
1.9
-0.1
Intensity (%)
0.5
5
50
500
5000
Size (d.nm)
MAPTMS
MAPTMS/Nb

Fig. 3

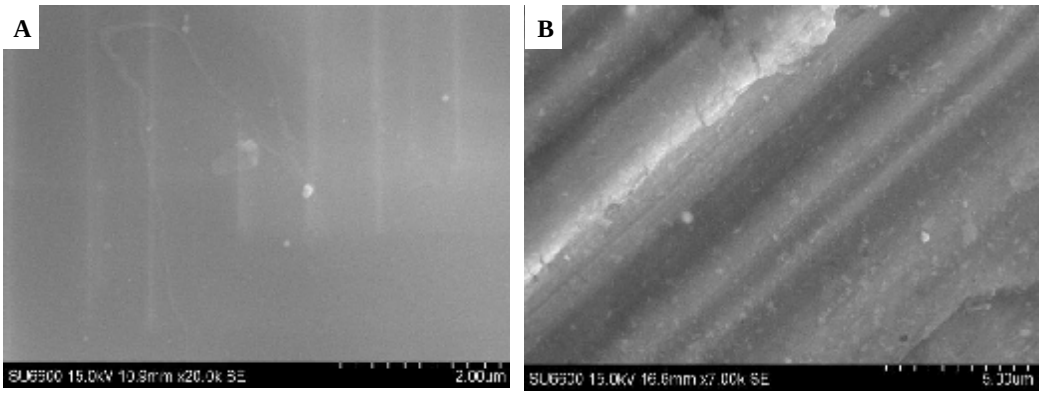
A
B
SU6500 15.0kV 10.9mm x20.0k SE
2.00um
SU6500 15.0kV 16.6mm x7.00k SE
5.00um

Fig. 4

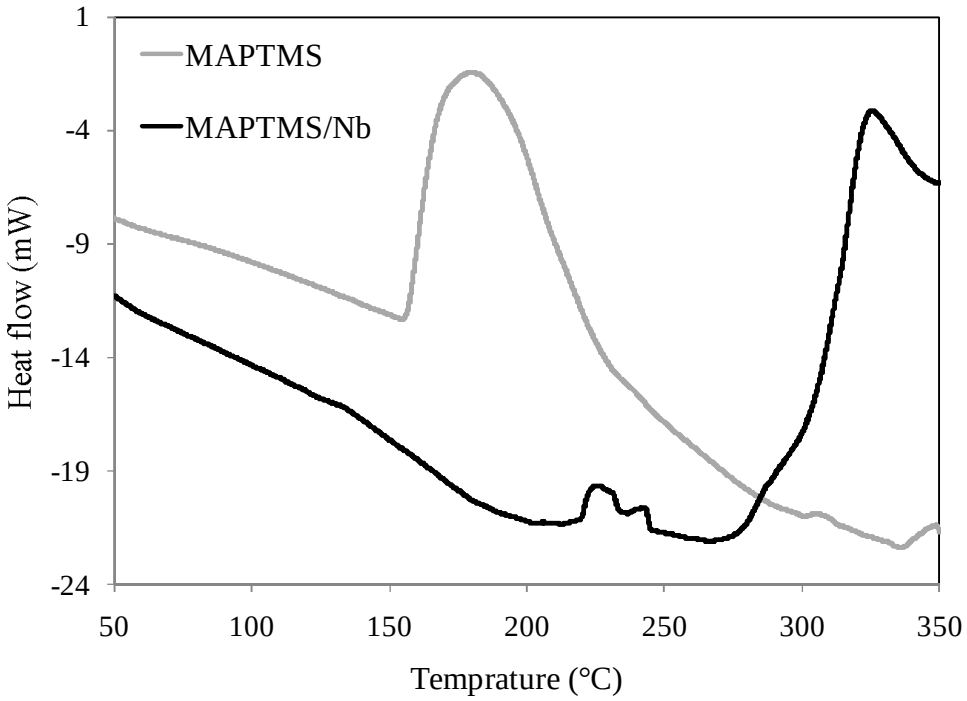
MAPTMS
MAPTMS/Nb
Heat flow (mW)
1
-4
-9
-14
-19
-24
50
100
150
200
250
300
350
Temprature (°C)

Fig. 5

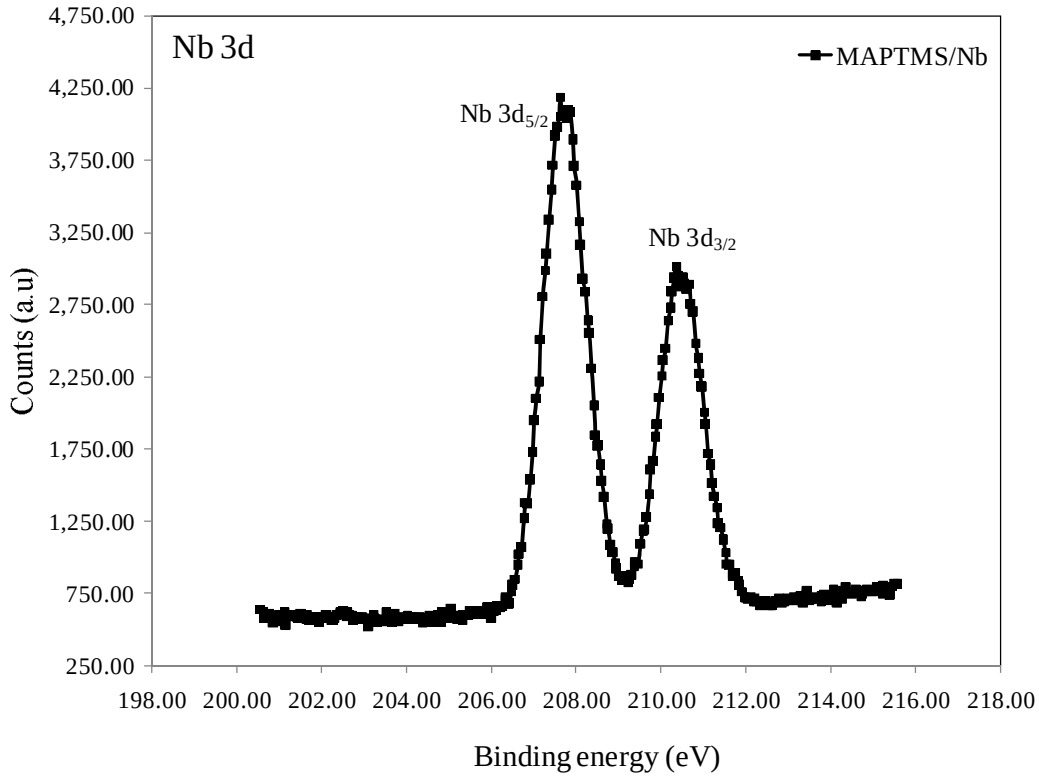
Nb 3d
MAPTMS/Nb
Nb 3d5/2
Nb 3d3/2
Counts (a.u)
4,750.00
4,250.00
3,750.00
3,250.00
2,750.00
2,250.00
1,750.00
1,250.00
750.00
250.00
198.00 200.00 202.00 204.00 206.00 208.00 210.00 212.00 214.00 216.00 218.00
Binding energy (eV)

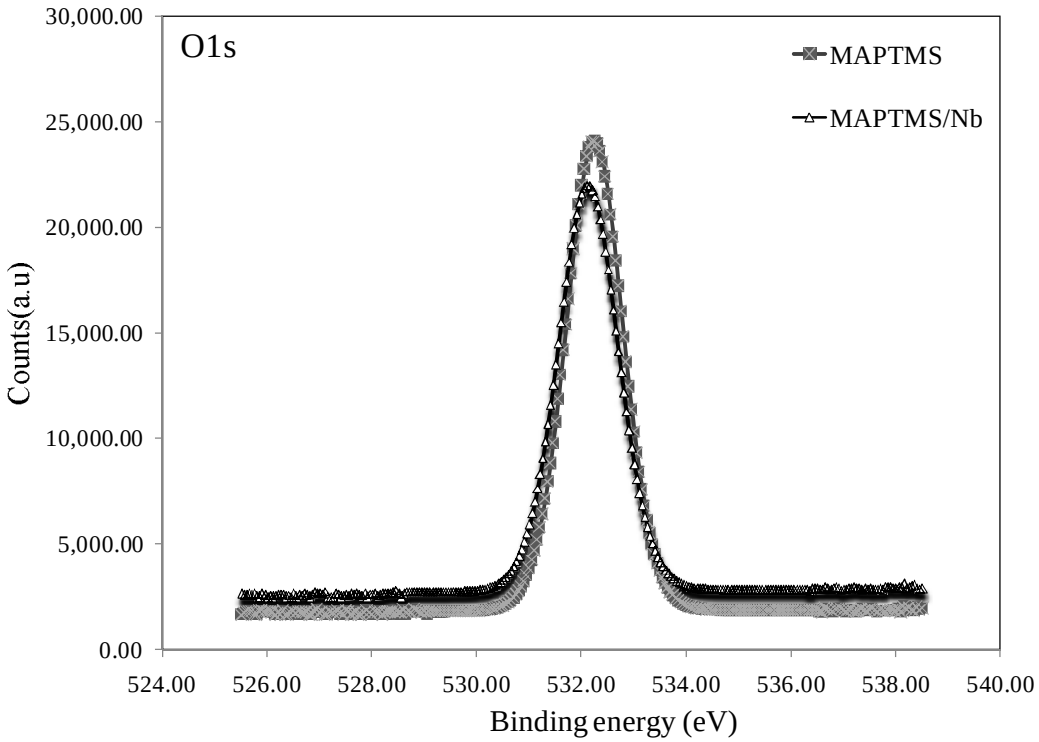
O1s
MAPTMS
MAPTMS/Nb
Counts(a.u)
30,000.00
25,000.00
20,000.00
15,000.00
10,000.00
5,000.00
0.00
524.00 526.00 528.00 530.00 532.00 534.00 536.00 538.00 540.00
Binding energy (eV)

Fig. 6(a)

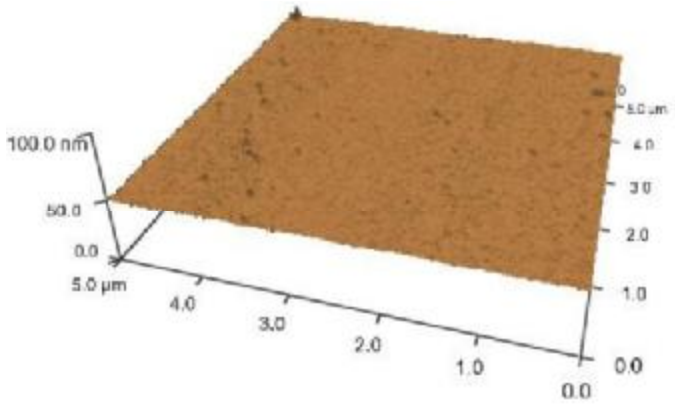

Fig. 6 (b)

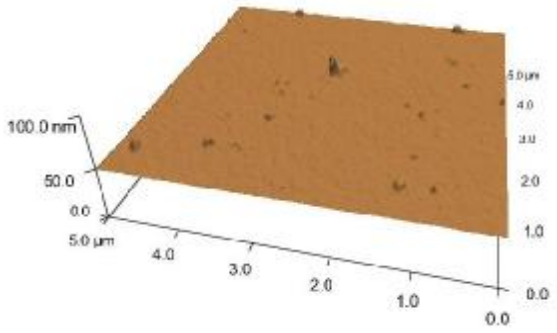

Fig.7 (a)

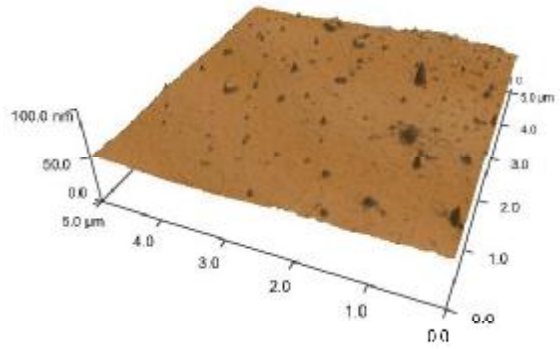

Fig 7 (b)

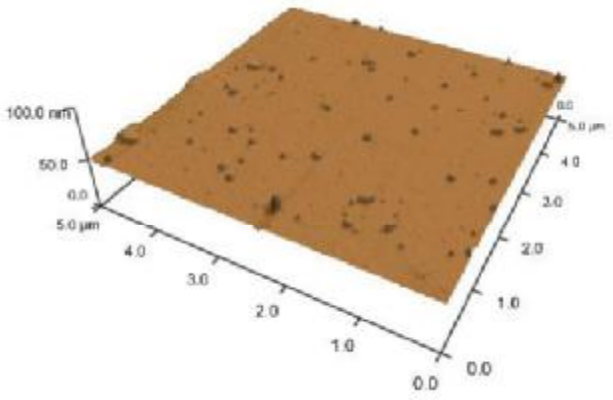

Fig. 8

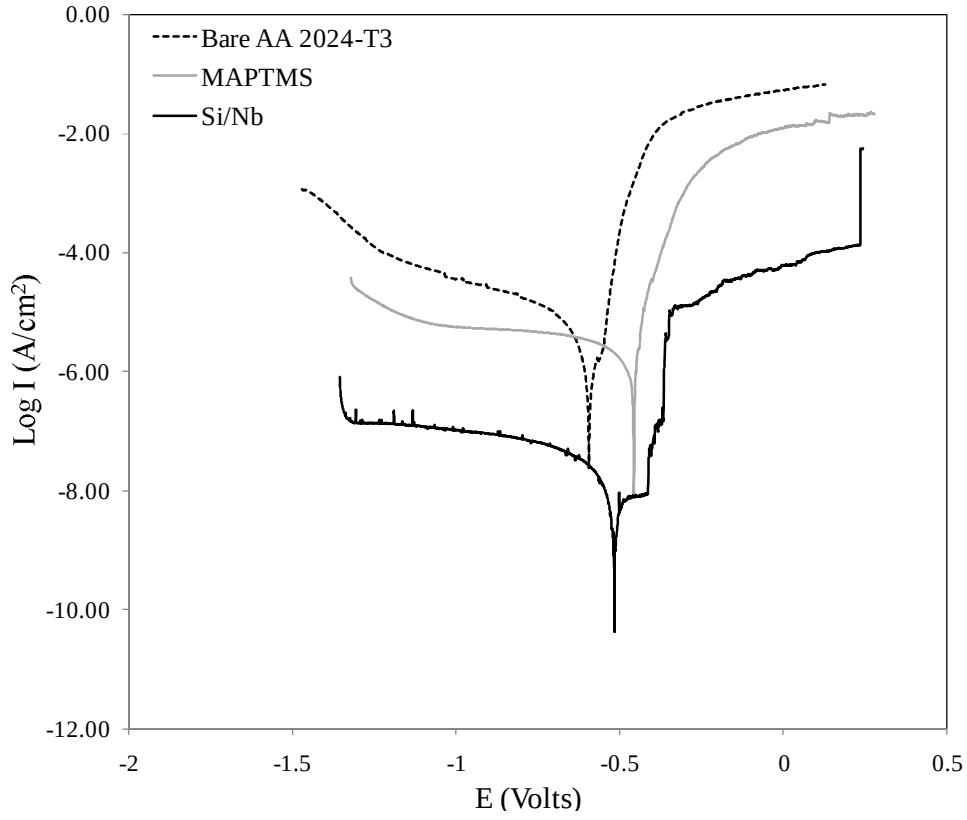
Bare AA 2024-T3
MAPTMS
Si/Nb
0.00
-2.00
-4.00
-6.00
-8.00
-10.00
-12.00
Log I (A/cm2)
-2
-1.5
-1
-0.5
0
0.5
E (Volts)

Fig. 9